Carbon 99 (2016) 267–271

Contents lists available at ScienceDirect

Carbon

journal homepage: www.elsevier.com/locate/carbon

Electrochemical charge storage in hierarchical carbon manifolds

Rajaram Narayanan [a], Hema Vijwani [c], Sharmila M. Mukhopadhyay [c], Prabhakar R. Bandaru [a, b, *]

[a] Department of Nanoengineering, University of California, San Diego, La Jolla, CA 92093, USA
[b] Program in Materials Science, Department of Mechanical and Aerospace Engineering, University of California, San Diego, La Jolla, CA 92093, USA
[c] Center for Nanoscale Multifunctional Materials, Wright State University, Dayton, OH 45435, USA

ARTICLE INFO

Article history:
Received 15 September 2015
Received in revised form
18 November 2015
Accepted 30 November 2015
Available online 8 December 2015

ABSTRACT

The use of hierarchical assemblies constituted from macroporous structures (*e.g.,* reticulated vitreous carbon, RVC) where the internal pore area is covered with closely spaced nanostructures (*e.g.,* carbon nanotubes, CNT) is proposed for substantially enhancing the energy density of electrochemical capacitors, while maintaining large charge/discharge rates. While the macroscale pores enable storage of substantial electrolyte volumes that would contribute through redox reactions to the energy density, the closely spaced nanostructures provide a large geometric area and capacitance in addition to enabling rate independent Faradaic charge storage via thin layer electrochemistry (TLE). A fifty fold increase in the double layer capacitance, in addition to increased Faradaic charge density – with potential for orders of magnitude improvement, was observed for the RVC-CNT electrodes, in comparison to the bare RVC foam electrode. It was seen that the hierarchical assembly enables the contribution from ~94% of the *net* volume of the wetted RVC-CNT electrode for active Faradaic charge storage.

1. Introduction

The notion of bridging the high energy density inherent to battery systems with the large power density available in electrostatic capacitors, in a hybrid device, has been a worthy goal of energy storage [1,2]. While electrochemical capacitors (ECs) have been invoked as the intermediary devices, the energy density is yet an order of magnitude smaller than competitive battery systems relegating the ECs mostly to power intensive applications [3–5]. Typically, EC electrodes are comprised of activated carbon (AC) with a large specific surface area, *SSA* (of up to 2000 m^2/g) available for electrostatic charge storage [6,7]. Recently, redox electrolytes in conjunction with AC electrodes have been proposed to improve the energy density of ECs [8–10]. Such electrolytes, in principle, could yield capacities comparable to that of batteries that use intercalation compounds such as transition metal oxides [11]. However, AC electrodes are not particularly suitable in conjunction with redox electrolytes as (a) their micro-porosity inhibits effective electrolyte penetration, and (b) they possess low specific pore volumes (of the order of 1 cm^3/g) resulting in the low utilization of redox species dissolved in solution [12].

In this article, we aim to suggest an alternate scheme for enhancing the energy density of EC devices. The basis for a concomitant enhancement in the energy density, while maintaining power capability, hinges on the use of hierarchical assemblies constituted from porous structures where the internal pore area is covered with closely spaced nanostructures [13–17]. The rationale for the use of such assemblies is to incorporate both macroscale pores (*e.g.,* of ~100 μm as in RVC) - which enable the storage of substantial electrolyte volumes that would contribute through redox reactions to the energy density, as well as nanostructures which provide a large geometric area and capacitance in addition to enhancing the rate of Faradaic processes, which is typically limited by species diffusion [18,19]. A relevant length scale, in this regard, is the equivalent diffusion layer thickness (d), over a given time (t), defined through:

$$d \sim \sqrt{\pi D t} \tag{1}$$

D is the diffusion coefficient of a relevant ion species [20]. When the nanostructure spacing or equivalent pore diameter (δ) is smaller than the d, conditions corresponding to thin layer electrochemistry (TLE) would be induced [21–23]. Battery-like energy

* Corresponding author. Program in Materials Science, Department of Mechanical Engineering, University of California, San Diego, La Jolla, CA 92093, USA.
E-mail address: pbandaru@ucsd.edu (P.R. Bandaru).

http://dx.doi.org/10.1016/j.carbon.2015.11.078
0008-6223/

densities may then be feasible through invoking TLE and Faradaic conditions in confined redox electrolytes, where the *net* obtainable charge would be proportional to the electrolyte *volume* (V_{el}) as well as the electrolyte concentration (C_o) by $Q = nFV_{el}C_o$, where n is the number of electrons per redox reaction, and F is the Faraday constant (= 96,485 C/mole). It should be noted that the underlying charge storage mechanism is not surface based, unlike traditional double-layer capacitors but is more related to the volume. Moreover, unlike batteries, the stored charge using such a scheme would possess the advantage of a large rate improvement, with large voltage scan rates.

2. Experimental section

2.1. Synthesis

The base porous structure is reticulated vitreous carbon (RVC) foam. It is commercially available from Ultramet Inc., and by itself had been earlier indicated as a promising electrode material for its ease of surface functionalization [24,25]. This grade of RVC foams (specified as 80 ppi: pores per inch, corresponding to ~ 31 pores/cm and an average pore size of 317.5 μm) has a specific surface area: *SSA* (per unit mass) of ~0.1 m^2/g and exhibits 97% porosity. Such pore size enables adequate gas passage and the synthesis of carbon nanotubes (CNTs), through chemical vapor deposition (CVD), on the pore walls: Fig. 1 [14]. While the detailed CNT synthesis has been described earlier [14], we discuss the procedure briefly. Vertically aligned nanotubes were synthesized onto the porous foams through a floating catalyst method, in a multi-zone CVD furnace reactor (MTI Corporation Ltd.). A mixture of ferrocene and xylene (catalyst and carbon source) was injected in the pre-heated zone maintained at 380 °C, which was followed by a reaction zone where the substrates were maintained at 700 °C in an Ar/H_2 environment. Subsequently, the furnace was allowed to cool down to room temperature in a reduced flow of Ar. The structural morphology of the as-fabricated CNT-foam hybrid structures was characterized by scanning electron microscopy (SEM: JEOL 7401F FE-SEM). The average CNT radius and height, for a growth time of ~40 min, were determined by SEM to be of the order of 9 ± 4 nm and 25 ± 3 μm, respectively. We report representative results on samples with a net CNT mass of ~6.7 mg in a volume of 1 cm^3 of RVC foam.

2.2. Electrochemical characterization

Cyclic voltammetry (CV) was performed, over a voltage range (ΔV) using a Gamry PCI4 potentiostat, to characterize the performance of the bare RVC (which served as the basis for comparison) as well as the hierarchically constituted RVC-CNT electrode, which formed the *working electrode* in a three-electrode setup (using Pt wire as the *counter electrode* and a saturated calomel electrode: SCE, as the *reference electrode*). We have verified explicitly, in our experimentation, that the counter electrode does not limit the current. The working electrodes were successively rinsed in acetone, isopropanol and distilled water prior to the electrochemical characterization to enhance electrode wetting. The double layer capacitance (C_{dl}) was estimated through the use of a KCl electrolyte (aq., 1 M), while the influence of redox reactions was probed through the addition of potassium hexacyanoferrate: $K_3Fe(CN)_6$ (with a species diffusion coefficient [26], $D = 6.8 \times 10^{-6}$ cm^2/s) to the 1 M KCl. Scan rates (ν) in the range of 0.001–2 V/s, were employed for the capacitance estimation. The C_{dl} was determined through the average of the ratio of the magnitude of the charge and discharge currents to the ν, through [27].

$$C_{dl} = \frac{\int_{V_i}^{V_f} \frac{IdV}{\nu}}{\Delta V \cdot 2m} \tag{2}$$

The I (= ½ [$|I_c| + |I_a|$]) denotes the voltammetric current taken as the average of the cathodic current: I_c, and the anodic current: I_a, with V_i and V_f being the initial and final voltages of the CV scan, and m is the measured electrode mass.

3. Results and discussion

At the very outset, the pore size in the bare RVC foam and that corresponding to the spacing between the CNTs are three orders of magnitude apart [13]. The CNT surface area of the sample (per unit volume) was deduced (on the basis of an average radius for an individual CNT of ~9 nm and a height of ~25 μm, discussed previously) to be of the order of ~17 m^2/g Consequently, a factor of ~170 (=17/0.1) increase was expected in the surface area due to the CNT growth within the RVC [14]. However, the specific capacitance of CNTs (which we experimentally determined to be ~5 $\mu F/cm^2$) is considerably smaller than that of glassy carbon constituting the RVC foam (~20 $\mu F/cm^2$) [28,29]. Consequently, a fifty fold increase in the volumetric capacitance, from ~0.8 mF/cm^3 for the bare RVC foam sample to ~40 mF/cm^3, for the RVC-CNT hierarchical electrode was observed through CV: Fig. 2(a). Based on the measured capacitance of the CNT foam, the equivalent surface area for the CNTs in the foam would be ~17.5 m^2/g, which is close to the previous estimate of ~17 m^2/g. Alternately, the gravimetric capacitance was determined to be of the order of 39.2 mF/cm^3 over the entire voltage range of ~0.8 V: Fig. 2(a), the charge density would be ~31.4 mC/cm^3. It should be noted that the C_{dl} was measured *only* in order to estimate the *SSA* of the structures electrochemically and that no formal comparison can be made between the C_{dl} and Faradaic capacity (from TLE) as they originate from different mechanisms.

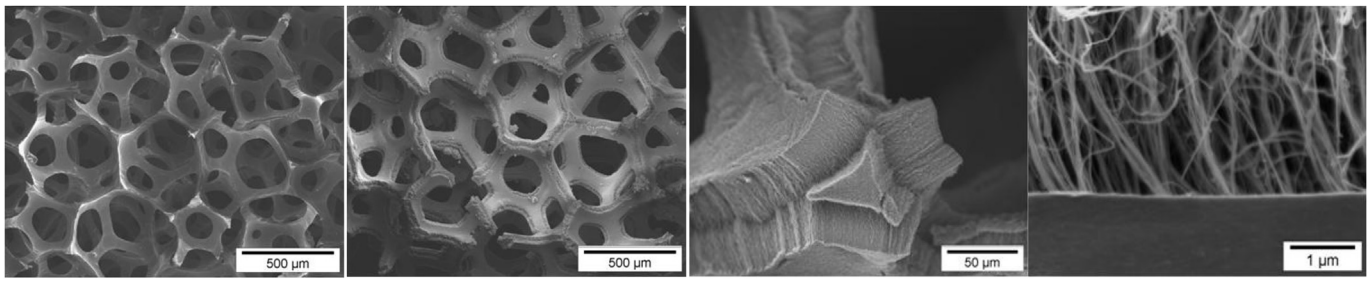

Fig. 1. Bare reticulated vitreous carbon (RVC) foam (*left*) was used as a template for the internal growth of carbon nanotubes (CNTs)- *figures on the right*, providing a hierarchical assemblage for energy storage. While the macroscale pores (*e.g.,* of ~300 μm as in RVC) enable the storage of electrolyte volumes that would contribute through redox reactions to the energy density, the nanostructures provide a large geometric area and capacitance in addition to limiting diffusion-related processes.

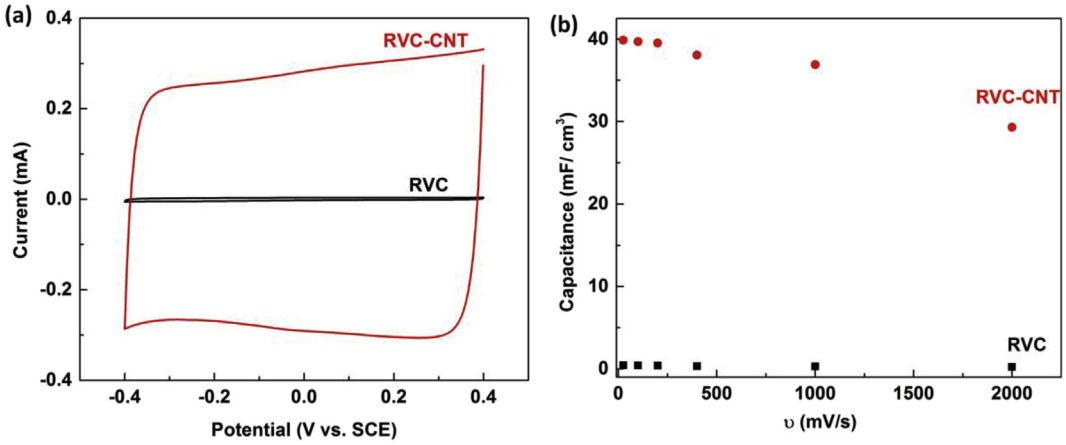

Fig. 2. (a) Cyclic voltammograms (CV: at 25 mV/s in 1 M KCl (aq.) electrolyte) indicating the fifty fold enhancement of the double layer current obtained from a *hierarchical* RVC-CNT electrode compared to a *bare* RVC foam electrode. (b) The variation of the double layer capacitance (C_{dl}) with the scan rate (v). (A color version of this figure can be viewed online)

However, while an ideal C_{dl} would be independent of the v, it was noted that there was a gradual decrease of the C_{dl} at $v > 1$ V/s: Fig. 2(b), possibly due to Ohmic effects [30]. Additionally, the *SSA* was estimated to be ~120 m^2/g, which is an order of magnitude lower than the state-of-the art and indicates that C_{dl} of the RVC-CNT manifold alone would be inadequate for applications requiring high energy density [31].

We had previously discussed that the use of TLE conditions, incorporating Faradaic redox reactions, would enable a much more significant enhancement of the energy density through increased charge storage while maintaining a rate comparable to that of double layer capacitors [23]. While the relevant redox reaction: $Fe(CN_6)^{4-} \rightleftharpoons Fe(CN_6)^{3-} + e^-$ would take place on the electrode/electrolyte interface, our investigations do not relate to surface phenomena specifically, but more to the prevalent TLE conditions. Fig. 3(a) indicates a representative voltammogram observed through the use of $K_3Fe(CN)_6$ (1 mM) in aq. KCl (1 M) on (a) RVC foam, and (b) RVC-CNT. In addition to the increased charge storage in the latter (evidenced by the larger peak currents), it was observed that the anode–cathode peak separation (ΔE_p) was smaller (53 mV for the RVC-CNT *vs.* 174 mV for the bare foam). Typically, a ΔE_p of less than ~59 mV is either indicative of TLE induced redox conditions or electrolyte adsorption on the surface [32]. The latter aspect was ruled out through transferring samples exposed to the $K_3Fe(CN)_6$ redox species to the bare electrolyte (1 M KCl), which resulted in a voltammetric response akin to that of a double layer capacitance without any redox peaks that could be associated with adsorption [23].

The redox peaks in the CV curves of Fig. 3 were analyzed for estimating the magnitude of the charge stored due to (i) the double-layer capacitance, as well as (ii) Faradaic reactions [33]. The results of such determination are depicted in Fig. 3 (b) and indicate that while the former contribution is relatively constant with the v, a sharp decrease was noted for the latter with v. The double-layer charge is roughly constant at 40 mC/cm^3. While the redox reaction induced charge seems to be of equivalent magnitude, it has the very important advantage that in principle the relevant charge density could be enhanced by orders of magnitude through the use of higher concentration redox electrolytes. For example, while 1 mM $K_3Fe(CN)_6$ was utilized in the present experiments, with the deployment of 1 M of redox couple, volumetric charge storage densities 1000 times larger could be obtained approaching battery-like capacities. Additionally, redox reactions involving multiple electron transfer would also help in further enhancing the capacity [34,35].

The *net* voltammetric charge (Q_{tot}), as estimated from the CV plots is due to contributions from both (a) planar diffusion limited current at the top of the electrode (I_{diff}) as well as in pores with radii >> d (equivalent to $\sqrt{\frac{\pi D \Delta V}{v}}$) and (b) a TLE current (I_{TLE}) in between the CNTs and in pores with radii << d: Fig. 4 (a).

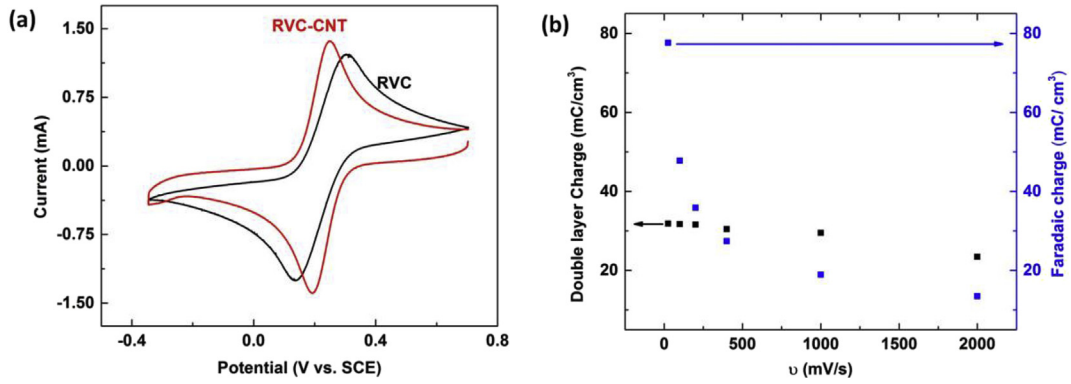

Fig. 3. (a) Cyclic voltammograms (at a scan rate of 25 mV/s) observed through the use of 1 mM $K_3Fe(CN)_6$ in 1 M KCl supporting electrolyte on (a) RVC foam, and (b) RVC-CNT electrodes. A lower anode–cathode peak separation (ΔE_p) was observed in the case of the RVC-CNT electrode. (b) The magnitude of the charge stored due to (i) C_{dl}, as well as the (ii) Faradaic reactions as a function of scan rate, as estimated from the CV scans of (a). (A color version of this figure can be viewed online)

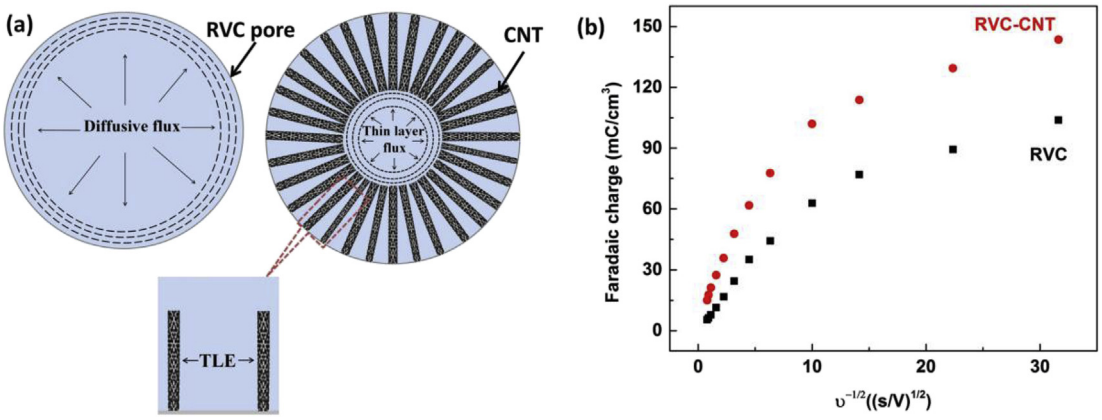

Fig. 4. (a) Compared to a bare RVC foam electrode (*left*), the RVC-CNT electrode (*right*), ion transport would have less diffusional limitations due to the easier establishment of thin layer electrochemistry (TLE) conditions. The CNTs induce TLE conditions both in the macropores of the RVC. (b) The variation of the total estimated charge: Q_{tot} with $\nu^{-1/2}$ for the RVC and RVC-CNT electrodes. The intercept on the ordinate axis would be related to the pore/electrolyte volume contributing to the energy density. (A color version of this figure can be viewed online)

Quantitatively:

$$Q_{tot} = Q_{diff} + Q_{TLE} = \frac{\int_{V_i}^{V_f}\left(I_{diff} + I_{TLE}\right)dV}{\nu}$$

$$= FA_{proj}C_o\left(\frac{\pi DF}{RT}\right)^{1/2}\int_{V_i}^{V_f}\chi\left(\frac{F\nu t}{RT}\right)\cdot\nu^{-1/2}dV + FV_{pore}C_o \qquad (3)$$

In Eq. (3), the scanned potential window is within the lower limit of V_i and the upper limit of V_f, and $\chi\left(\frac{F\nu t}{RT}\right)$ denotes the normalized current for a reversible reaction under planar diffusion. It was noted that the consideration of the charge is preferred over the peak currents, as the latter are susceptible to Ohmic resistance related anomalies as well as the overlap of peaks from the diffusion and TLE related processes [36,37]. Additionally, the intercept of the observed plots-as in Fig. 4(b), of Q_{tot} with $\nu^{-1/2}$ ($= FV_{pore}C_o$) would be related to the contributing pore volume (V_{pore}) in the given ν range, and governed by TLE conditions [38]. Ideally, $V_{pore} = V_{el}$, implying complete utilization of the inner volume of the hierarchical manifold by the electrolyte.

As expected, it was observed that generally the Faradaic charge for the RVC-CNT electrode was larger than that of the bare RVC foam for the investigated ν. The variation with the $\nu^{-1/2}$ was nonlinear indicating a range of length scales, which may be estimated through a piece-wise fitting of the curves. The extrapolation of such fits to a $\nu^{-1/2} \rightarrow 0$ would be representative of very large scan rates where diffusion would play a negligible role and the charge capacity would mainly arise from TLE conditions [38]. Generally, an overlap of the diffusion layers relevant to each CNT in an array occurs as the ν decreases resulting in planar diffusion to the top of the electrode. However, inside the pores, a decreased concentration gradient results in thin layer behavior at lower ν, and more of the electrolyte volume can be accessed.

Consequently, from the intercept value ($= FV_{pore}C_o$), the relevant contributing volumes (V_{pore}) as well as the length scales may be determined. The results of such extrapolation are indicated in Fig. 5, where the ordinate indicates the percentage of the total volume of the RVC-CNT electrode that is being harnessed for charge storage. It was observed that at low ν, most of the charge is accessed through TLE mechanisms and close to 94% of the *net* volume of the wetted RVC-CNT electrode contributes. However, for the bare RVC foam, only ~60% of the *net* volume is active for charge storage.

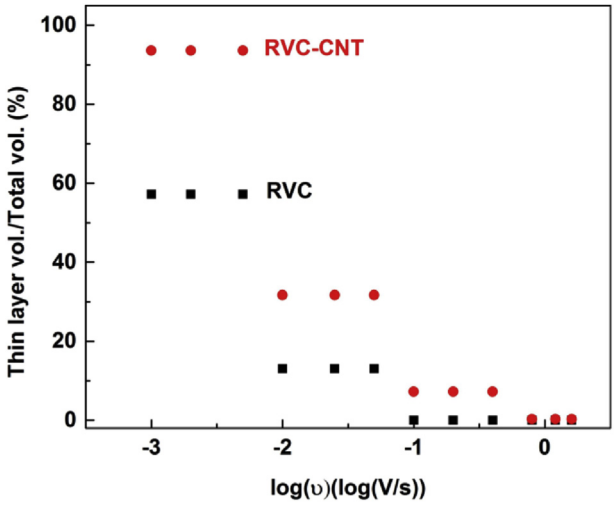

Fig. 5. The percentage of the total volume of the RVC-CNT electrode that is being harnessed for charge storage. While at low ν, most of the charge is accessed through TLE mechanisms and close to 94% of the *net* volume of the wetted RVC-CNT electrode contributes, for the bare RVC foam, only ~60% of the *net* volume seems to be active for charge storage. (A color version of this figure can be viewed online)

Consequently, it may be surmised that the role of the CNTs synthesized within the RVC foam, in addition to increasing the effective surface area of the manifold, is to diminish the effective pore size of the native RVC foam and enable a greater access to the electrolyte volume. This may be seen through an application of Eq. (3), with $D = 6.8 \times 10^{-6}$ cm^2/s *and* $\nu = 1$ mV/s, yielding a d ~230 μm, while the pore size (δ) is of the order of 320 μm, implying the absence of TLE conditions. However, with the growth of 25 μm long CNTs, the effective pore size (δ) is reduced to 270 μm indicating a greater likelihood of achieving TLE in the RVC-CNT manifold and access to the enclosed electrolyte. It should also be noted that the presence of CNTs induce TLE conditions due to electrolytes trapped in between, resulting in enhanced mass transport in the circumferential direction. Given that the proof-of-concept experiments were done with 1 mM $K_3Fe(CN)_6$, there is enormous promise for further enhancing the charge capacity, which is linearly proportional to the concentration of the redox species. For example, using redox additives with a greater solubility, *e.g.,* KI, with a solubility limit of ~8 M may enhance the charge storage capacity potentially

by a factor of 8000.

4. Conclusion

In summary, this work proposes the use of hierarchical porous manifolds for *both* large energy density - through redox electrolytes stored at a macro-pore level, and power density - using high surface area nanostructures. Such a scheme accomplishes the dual objectives of minimizing the issue of inadequate charge storage in electrochemical capacitors, and that of diffusional limitations, which limit the power of batteries.

Acknowledgments

P. R. Bandaru acknowledges the financial support (through CMMI 1246800) of the National Science Foundation (NSF) and the Defense Advanced Research Projects Agency (DARPA: W911NF-15-2-0122). Wright State team acknowledges support of the National Science Foundation (NSF-CBET-1449582), the U.S. Environmental Protection Agency, and Ohio Third Frontier. Equipment support from NSF-MRI award and Ohio Board of Regents is acknowledged. The authors thank Ultramet Inc. for generous supply of reticulated carbon foams. Discussions with H. Yamada are deeply appreciated.

References

[1] J.B. Goodenough, Y. Kim, Challenges for rechargeable Li batteries †, Chem. Mater. 22 (2010) 587–603, http://dx.doi.org/10.1021/cm901452z.
[2] A. Manthiram, Materials challenges and opportunities of lithium ion batteries, J. Phys. Chem. Lett. 2 (2011) 176–184, http://dx.doi.org/10.1021/jz1015422.
[3] J.R. Miller, A.F. Burke, Electrochemical capacitors: challenges and opportunities for real-world applications, Electrochem. Soc. Interface (2008) 53–57.
[4] J.R. Miller, Valuing reversible energy storage, Sci. (80-) 335 (2012) 1312–1313.
[5] J.M. Miller, Ultracapacitor Applications, The Institution of Engineering and Technology, Herts, UK, 2011.
[6] J. Chmiola, G. Yushin, Y. Gogotsi, C. Portet, P. Simon, P.L. Taberna, Anomalous increase in carbon capacitance at pore sizes less than 1 nanometer, Science 313 (2006) 1760–1763, http://dx.doi.org/10.1126/science.1132195.
[7] D. Qu, H. Shi, Studies of activated carbons used in double-layer capacitors, J. Power Sources 74 (1998) 99–107.
[8] K. Fic, E. Frackowiak, F. Béguin, Unusual energy enhancement in carbon-based electrochemical capacitors, J. Mater. Chem. 22 (2012) 24213, http://dx.doi.org/10.1039/c2jm35711a.
[9] M. Meller, J. Menzel, K. Fic, D. Gastol, E. Frackowiak, Electrochemical capacitors as attractive power sources, Solid State Ion. 265 (2014) 61–67, http://dx.doi.org/10.1016/j.ssi.2014.07.014.
[10] S.T. Senthilkumar, R.K. Selvan, Y.S. Lee, J.S. Melo, Electric double layer capacitor and its improved specific capacitance using redox additive electrolyte, J. Mater. Chem. A 1 (2013) 1086, http://dx.doi.org/10.1039/c2ta00210h.
[11] V. Augustyn, P. Simon, B. Dunn, Pseudocapacitive oxide materials for high-rate electrochemical energy storage, Energy Environ. Sci. 7 (2014) 1597, http://dx.doi.org/10.1039/c3ee44164d.
[12] G. Salitra, A. Soffer, L. Eliad, Y. Cohen, D. Aurbach, Carbon electrodes for double-layer capacitors I. Relations between ion and pore dimensions, J. Electrochem. Soc. 147 (2000) 2486, http://dx.doi.org/10.1149/1.1393557.
[13] S.M. Mukhopadhyay, A. Karumuri, I.T. Barney, Hierarchical nanostructures by nanotube grafting on porous cellular surfaces, J. Phys. D Appl. Phys. 42 (2009) 195503, http://dx.doi.org/10.1088/0022-3727/42/19/195503.
[14] H. Vijwani, M.N. Nadagouda, V. Namboodiri, S.M. Mukhopadhyay, Hierarchical hybrid carbon nano-structures as robust and reusable adsorbents: kinetic studies with model dye compound, Chem. Eng. J. 268 (2015) 197–207, http://dx.doi.org/10.1016/j.cej.2015.01.027.
[15] N. Liu, Z. Lu, J. Zhao, M.T. McDowell, H.-W. Lee, W. Zhao, et al., A pomegranate-inspired nanoscale design for large-volume-change lithium battery anodes, Nat. Nanotechnol. 9 (2014) 187–192, http://dx.doi.org/10.1038/nnano.2014.6.
[16] I.T. Barney, D.S.R. Lennaerts, S.R. Higgins, S.M. Mukhopadhyay, Specific surface area of hierarchical graphitic substrates suitable for multi-functional applications, Mater. Lett. 88 (2012) 160–163, http://dx.doi.org/10.1016/j.matlet.2012.08.042.
[17] Y. Guo, Z. Shi, M. Chen, C. Wang, Hierarchical porous carbon derived from sulfonated pitch for electrical double layer capacitors, J. Power Sources 252 (2014) 235–243, http://dx.doi.org/10.1016/j.jpowsour.2013.11.114.
[18] J.A. Nichols, H. Saito, C. Deck, P.R. Bandaru, J.A. Nichols, H. Saito, et al., Artificial introduction of defects into vertically aligned multiwalled carbon nanotube ensembles : application to electrochemical sensors artificial introduction of defects into vertically aligned multiwalled carbon nanotube ensembles : application to ele, J. Appl. Phys 102 (2014) 064306, http://dx.doi.org/10.1063/1.2783945.
[19] K.R. Ward, L. Xiong, N.S. Lawrence, R.S. Hartshorne, R.G. Compton, Thin-layer vs. semi-infinite diffusion in cylindrical pores: a basis for delineating Fickian transport to identify nano-confinement effects in voltammetry, J. Electroanal. Chem. 702 (2013) 15–24, http://dx.doi.org/10.1016/j.jelechem.2013.05.005.
[20] R.G. Compton, C.E. Banks, Understanding Voltammetry, Imperial College Press, London, UK, 2011.
[21] A.T. Hubbard, F.C. Anson, The theory and practice of electrochemistry with thin layer cells, Electroanal. Chem. A Ser. Adv. (1970) 129–214.
[22] E.O. Barnes, X. Chen, P. Li, R.G. Compton, Voltammetry at porous electrodes: a theoretical study, J. Electroanal. Chem. 720–721 (2014) 92–100, http://dx.doi.org/10.1016/j.jelechem.2014.03.028.
[23] R. Narayanan, P.R. Bandaru, High rate capacity through redox electrolytes confined, J. Electrochem. Soc. 162 (2015) A86–A91, http://dx.doi.org/10.1149/2.0461501jes.
[24] J.M. Friedrich, C. Ponce-de-León, G.W. Reade, F.C. Walsh, Reticulated vitreous carbon as an electrode material, J. Electroanal. Chem. 561 (2004) 203–217, http://dx.doi.org/10.1016/j.jelechem.2003.07.019.
[25] J. Wang, Reticulated vitreous carbon—a new versatile electrode material, Electrochim. Acta 26 (1981) 1721–1726, http://dx.doi.org/10.1016/0013-4686(81)85156-0.
[26] S.J. Konopka, B. McDuffie, Diffusion coefficients of ferri- and ferrocyanide ions in aqueous media, using twin-electrode thin-layer electrochemistry, Anal. Chem. 42 (1970) 1741–1746.
[27] M.D. Stoller, S. Park, Y. Zhu, J. An, R.S. Ruoff, Graphene-based ultracapacitors, Nano Lett. 8 (2008) 3498–3502, http://dx.doi.org/10.1021/nl802558y.
[28] H. Yamada, P.R. Bandaru, Limits to the magnitude of capacitance in carbon nanotube array electrode based electrochemical capacitors, Appl. Phys. Lett. 102 (2013) 173113, http://dx.doi.org/10.1063/1.4803925.
[29] a. Braun, M. Bärtsch, O. Merlo, B. Schnyder, B. Schaffner, R. Kötz, et al., Exponential growth of electrochemical double layer capacitance in glassy carbon during thermal oxidation, Carbon N. Y. 41 (2003) 759–765, http://dx.doi.org/10.1016/S0008-6223(02)00390-1.
[30] W.G. Pell, B.E. Conway, Voltammetry at a de Levie brush electrode as a model for electrochemical supercapacitor behaviour, J. Electroanal. Chem. 500 (2001) 121–133.
[31] P. Simon, Y. Gogotsi, Materials for electrochemical capacitors, Nat. Mater. 7 (2008) 845–854.
[32] B.E. Conway, Transistion from “Supercapacitor” to “Battery” behavior in electrochemical energy storage, J. Electrochem. Soc. 138 (1991) 1539–1548.
[33] M. Hoefer, P.R. Bandaru, Determination and enhancement of the capacitance contributions in carbon nanotube based electrode systems, Appl. Phys. Lett. 95 (2009) 183108.
[34] S. Roldan, M. Granda, R. Men, R. Santamaría, C. Blanco, R. Menendez, et al., Mechanisms of energy storage in carbon-based supercapacitors modified with a quinoid redox-active electrolyte, J. Phys. Chem. C 115 (2011) 17606–17611, http://dx.doi.org/10.1021/jp205100v.
[35] E. Frackowiak, K. Fic, M. Meller, G. Lota, Electrochemistry serving people and nature: high-energy ecocapacitors based on redox-active electrolytes, ChemSusChem 5 (2012) 1181–1185, http://dx.doi.org/10.1002/cssc.201200227.
[36] Fedkiw, S. Peter, J.W. Weidner, Ohmic distortion of reversible waves in thin layer cells, Electrochim. Acta 33 (1988) 421–424.
[37] M.C. Henstridge, E.J.F. Dickinson, R.G. Compton, Mass transport to and within porous electrodes. Linear sweep voltammetry and the effects of pore size: the prediction of double peaks for a single electrode process, Russ. J. Electrochem. 48 (2012) 629–635, http://dx.doi.org/10.1134/S1023193512060043.
[38] V. Augustyn, J. Come, M.A. Lowe, J.W. Kim, P.-L. Taberna, S.H. Tolbert, et al., High-rate electrochemical energy storage through Li+ intercalation pseudocapacitance, Nat. Mater. 12 (2013) 518–522, http://dx.doi.org/10.1038/nmat3601.